AAPS PharmSciTech, Vol. 13, No. 2, June 2012 (© 2012)
DOI: 10.1208/s12249-012-9767-6

Research Article

Ligustrazine Phosphate Ethosomes for Treatment of Alzheimer's Disease, *In Vitro* and in Animal Model Studies

Jun Shi,[1,2] Yiming Wang,[2] and Guoan Luo[1,2,3]

Received 19 April 2011; accepted 28 February 2012; published online 14 March 2012

Abstract. In the present study, we have investigated transdermal administration of ligustrazine phosphate (LP), as an antioxidant, for the treatment of Alzheimer's disease (AD). The LP transdermal ethosomal system was designed and characterized. Franz-type diffusion cells and confocal laser scanning microscopy were used for the *in vitro* permeation studies. Furthermore, the effect of LP transdermal ethosomal system on AD was evaluated in the scopolamine-induced amnesia rats by evaluating the behavioral performance in the Morris water maze test. The activities of the antioxidant enzymes and the levels of the lipid peroxidation product malondialdehyde (MDA) in the brain of rats were also determined. The results showed that both the penetration ability and the drug deposition in skin of the LP ethosomal system were significantly higher than the aqueous one. The LP transdermal ethosomal system could recover the activities of the antioxidant enzymes and the levels of MDA in the brain of the amnesic rats to the similar status of the normal rats, which was also indirectly reflected by the improvement in the behavioral performance. In conclusion, LP might offer a potential alternative therapeutic drug in the fight against AD, and ethosomes could be vesicles of choice for transdermal delivery of LP.

KEY WORDS: Alzheimer's disease; ethosome; ligustrazine phosphate; scopolamine; transdermal delivery.

INTRODUCTION

Alzheimer's disease (AD) is a progressive neurodegenerative disease with piecemeal loss in memory, which mostly affects the elderly population (1). The pathophysiology of AD is complex including the deposition of the senile plaques mainly composed of amyloid beta protein, neurofibrillary tangles in patients' brain (2,3), abnormalities of cholinergic and the potential involvement of oxidative stress and inflammatory (4). These factors may interact and amplify each other in a vicious cycle of toxicity leading to neuronal dysfunction, cell dysfunction, and finally cell death (5). Notably, it has been reported that the oxidative stress is perhaps the earliest feature of AD (6), which means the free radicals play an important role in the progression of AD. According to the free radical theory (7), the generation of reactive oxygen species (ROS) or free radicals can lead to cell and tissue damage, resulting in aging and untimely cell apoptosis, which are both involved in the pathogenesis of AD. The ROS can be scavenged by endogenous antioxidants including superoxide dismutase (SOD) and glutathione peroxidase (GSH-Px). Malondialdehyde (MDA) is a by-product of lipid peroxidation induced by free radicals and is widely used as a biomarker of oxidative stress (8). One approach against ROS in neurodegenerative disorders is to enhance oxidative defenses via antioxidants (7). In this respect, there are numerous reports on the use of antioxidant as alternative treatments for AD syndromes (9,10).

Ligustrazine, an alkaloid extracted from the Chinese herbal medicine, Haoben Chuanxiong (*Ligusticum chuanxiong Hort*), has been widely used in the treatment of cerebrovascular and cardiovascular diseases in clinic, such as myocardial and cerebral infarction (11). In animal studies, ligustrazine can improve myocardial infarction syndrome (12) and reduce cerebral ischemic reperfusion damage (13). Furthermore, several animal and cellular studies have demonstrated that ligustrazine plays a protective role in the improvements of learning and cognitive function, the possible mechanisms of which include inhibitory effects on the calcium overload, anti-apoptotic activity, and anti-inflammatory potential (14,15). Recent studies have proved that ligustrazine (100 mg/kg, i.g.) can significantly improve the hippocampal cholinergic system function, attenuate oxidative damage, and therefore remarkably enhance the learning and memory abilities in D-galactose-induced AD mice model (16), suggesting that ligustrazine may become a novel drug candidate for the treatment of AD.

Additionally, ligustrazine phosphate (LP) is the synthetic product of ligustrazine, and the structure of LP is shown in Fig. 1. LP with the small molar mass of 252.21 has satisfied penetration through the blood–brain barrier (17). LP oral or injection administration has a number of disadvantages. LP, given orally to humans, undergoes extensive hepatic first-pass metabolism, leading to a low oral bioavailability (10–30%) and a very

[1] School of Pharmacy, East China University of Science and Technology, Shanghai 200237, People's Republic of China.
[2] Department of Chemistry, Tsinghua University, Beijing 100084, People's Republic of China.
[3] To whom correspondence should be addressed. (e-mail: luoga@tsinghua.edu.cn)

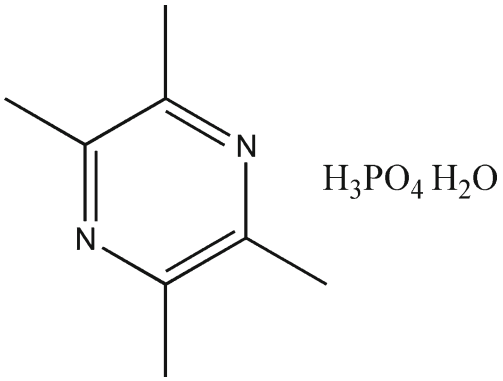

Fig. 1. Structure of ligustrazine phosphate

short elimination half-life (0.5–2 h) (18), which needs to be administered frequently (100 mg three times daily) resulting in variable absorption profiles. Moreover, LP injection needs to be administered by intravenous drip infusion over 3 to 4 h once daily, which may not only reduce patient compliance but also lead to possible cumulative toxicosis, such as cerebrovascular and cardiovascular lesions and allergic reactions (19). The drawbacks of the oral or injection drug administration can be offset by the transdermal administration, which can avoid the first-pass metabolism, maintain the relatively stable plasma drug concentration, reduce the dosage interval, and enhance patient compliance (20,21). On the other hand, LP is a hydrophilic molecule that has limited skin permeability to achieve therapeutic blood concentrations. For this reason, ethosome as an enhancing permeation carrier was adopted to overcome the difficulties of the skin permeability. Ethosomes as novel liposomal delivery systems, containing soft phospholipid vesicles in the presence of high concentrations of ethanol, are able to deliver permeates into the deep layers of the skin and across the skin in terms of both quantity and depth, which hence appear to be vesicles of choice for transdermal drug delivery (22,23).

One hypothesis tested in this work was that LP could be efficient in treating AD syndromes through affecting the oxidative system in the brain, since there are few literatures referring to the anti-amnesic efficiency of LP and the pharmacological mechanisms have been still poorly understood. Therefore, the present work focused on the characteristics of LP ethosomes and their *in vitro* skin permeation behavior. Furthermore, the pharmacodynamic study was also carried out to evaluate the efficiency of LP transdermal administration in scopolamine-induced amnesia rats.

MATERIALS AND METHODS

Drugs and Reagents

Ligustrazine phosphate (LP, purity>98.0%) was purchased from Yanjing Pharmaceutical Company (Beijing, China). Egg phosphatidylcholine (Lipoid E PC®, 99.1% pure) was bought from Lipoid GmbH (Ludwigshafen, Germany). Rhodamine 6G (R6G) was obtained from Aladdin Chemical Reagent Co., Ltd (Shanghai, China). Carbomer 940 was purchased from Caelo (Hilden, Germany). Scopolamine hydrochloride was purchased from Sigma–Aldrich (St Louis, MO, USA) and dissolved in 0.9% saline at the concentration of 0.6 mg/ml.

Preparation of LP Vesicular Systems

LP ethosomal systems containing 1.15% (*w*/*w*) drug, 2.5% (*w*/*w*) egg phosphatidylcholine, and 30% ethanol in carbomer gel were used in this work. The systems were prepared as follows: the aqueous solution of the drug was added slowly in a fine stream with constant mixing at 700 rpm to the ethanolic solution of egg phosphatidylcholine, and the vesicle suspension was dispersed by a probe sonicator (Scientz Biotechnology Co. Ltd., Ningbo, China) at 50% amplitude for 3 min. The mixture was then added to a 1.0% carbomer gel to obtain the final ethosomal system. LP aqueous system containing the same concentrations of drug and ethanol in 1.0% carbomer gel was used as the control system. For confocal laser scanning microscopy (CLSM) studies, LP ethosomal systems and the control systems were labeled with 0.01% R6G (as a fluorescence probe), respectively.

Physical Characterization of LP Vesicular Systems

Measurements of Vesicle Size, Size Distribution, and pH Value

The vesicle size and size distribution of ethosomes were determined by laser scattering (Zetasizer 3000 HS, Malvern Instruments, UK), and the determination was repeated in triplicate. In order to evaluate the stability of ethosomes, the size and size distribution of ethosomes were measured after being stored at 4°C for 4 weeks. The pH value of the LP ethosomal system was measured using the microprocessor pH meter (pH213, Hanna Instruments, Italia).

Determination of Entrapment Efficiency

The entrapment efficiency of the LP ethosomes was determined by the ultracentrifugation method. An aliquot of 0.5 ml LP ethosomes was centrifuged at 40,000 rpm for 3 h at 4°C (24). Following centrifugation, the supernatant was collected and the amount of unentrapped LP in the supernatant was determined by high-performance liquid chromatography (HPLC). To determine the total amount of LP in ethosomes, an aliquot of 1.0 ml 10% (*v*/*v*) Triton X-100 in ethanol for emulsion breaking was added to 0.5 ml LP ethosomes, and the mixture was diluted to 10 ml with acetonitrile-water (22:78, *v*/*v*). Thereafter, the concentration of LP was assayed by HPLC. The entrapment efficiency was calculated using the following equation: $[(T-S)/T]\times 100(\%)$, where T is the total amount of LP in ethosomes and S is the amount of unentrapped drug in the supernatant.

CLSM Studies

The depth of skin penetration from R6G loaded ethosomal systems was investigated by means of CLSM. LP ethosomal system (2.0 g) and LP aqueous system (2.0 g) labeled with R6G were applied nonocclusively for 12 h on full-thickness defrosted nude mice (ICR) in Franz-type diffusion cells (TPY-2 diffusion test apparatus, Shanghai Huanghai Drug Control Instrument Co. Ltd., Shanghai, China), respectively, and 10 mM phosphate buffer (pH 7.4) was used as the receptor medium. At the end of the experiment, the excess of the preparation was carefully wiped from the skin surface and the treated area was freezing sliced into pieces. The skin was optically scanned at 25-μm increments through the *Z*-axis with

a Zeiss Observer. Z1 microscope attached to a universal Zeiss fluorescence microscope having air plan 40×0.95 NA objective lens. Optical excitation was carried out with a 543-nm He–Ne laser beam and fluorescence emission was detected above 560 nm. Relative fluorescence intensity of the probe (arbitrary units) in the skin was further assessed using a Zeiss computerized program (Zen 2009 light edition). Pinhole size, electron gain, neutral density filters, and background level were set up at the beginning of the experiment and were kept constant during florescence measurements.

In Vitro Skin Permeation Study

The abdominal skins of male Sprague–Dawley rats (200± 20 g) were used for the experiments, and the *in vitro* permeation studies were performed in Franz-type diffusion cells with an effective diffusion area of 2.32 cm^2 and a receptor volume of 6.5 ml. Ten millimolars phosphate buffer (pH 7.4) was used as the receptor medium, which was magnetically stirred at 37±0.5°C with a constant rate of 600 rpm during the experiment. LP ethosomal system (2.0 g) and LP aqueous system (2.0 g) were applied on the donor side, respectively. At predetermined time, 200 μl of the receptor medium was withdrawn and replaced with an equal volume of freshly prepared medium. The samples were centrifuged for 15 min at 13,000 rpm and an aliquot (10 μl) of the supernatant was analyzed by HPLC to determine the drug concentration. Experiments were replicated in triplicate. The electrical resistance of the skin was assessed before and after the experiment to monitor the skin integrity. The resistance values did not change significantly, indicating that the skin integrity was maintained during the 24-h permeation study.

At the end of the experiment (24 h), the skin was washed with a cotton pad wetted with acetone, weighted, and homogenized in ice-cold saline at 13,000 rpm in a Potter homogenizer. The homogenate was centrifuged at 3,500 rpm at 4°C for 15 min, and the supernatant was collected. To 500 μl of the supernatant, 300 μl of 0.01 mol/l NaOH aqueous solution, 1 ml of methanol and 2 ml of dichloromethane were added. The mixture was then vortexed for 5 min and centrifuged for 10 min at 4,000 rpm. The organic phase was transferred to another tube, acidified with 400 μl of 0.05 mol/l HCl–methanol solution, and vortexed for 1 min. The supernatant was evaporated to dryness under a stream of nitrogen and the residue was reconstituted in 200 μl of purified water. Twenty microliters of the obtained samples were determined by HPLC.

Cumulative corrections were made to obtain the total amount of LP permeated at each time interval. The cumulative amount (Q, micrograms per square centimeter) of LP permeated through the rat skin was plotted as a function of time. The permeation rate of LP at steady-state (J_s, micrograms per square centimeter per hour) was calculated from the slope of linear portion of the cumulative amount permeated through the rat skin per unit area *versus* time plot. The lag time (T_{lag}, hour) was calculated from the X-intercept of the linear portion of the plot.

HPLC Analytical Conditions for LP Determination

LP was analyzed by reversed phase HPLC using Hitachi's model L-2300 HPLC system (Tokyo, Japan). The HPLC system consisted of a quaternary pump (L-2130, Hitachi, Japan), a UV detector (L-2400, Hitachi, Japan), an automatic injector (L-2200, Hitachi, Japan) and a workstation. The column was an Agilent TC-C18 column (4.6×250 mm, 5 μm). The mobile phase consisted of a binary mixture of acetonitrile and 0.01 % triethylamine solution (22:78, *v*/*v*) flowing at 1.0 ml/min. The detection wavelength was set at 301 nm, and the retention time was about 9.3 min. The assay was linear in the concentration range of 0.5–500.0 μg/ml, and the limit of detection was 0.001 μg. The correlation coefficient of the standard curve was 0.999.

Pharmacodynamic Studies

Animals and Drug Administration

Animal experiments were conducted in full compliance with the Institutional Animal Care and Use Committee of Tsinghua University (Beijing, China). Animals were housed under standard 12-h light/dark cycle and a temperature of 25°C, with food and water freely available. Eighteen male Sprague–Dawley rats, weighing 230–270 g, were randomly assigned to three groups (six rats for each group): groups I–III, respectively. Two days before the experiment, the hair of the abdominal skin was shaved with an electric clipper. The rats in groups I and II were transdermally administered with the empty ethosomal system without drug in every 3 days for nine consecutive days, as a control and a model, respectively. The rats in group III were transdermally administered with the LP ethosomal system (113 mg/kg), which was applied nonocclusively on 28 cm^2 of the abdominal skin, in every 3 days for nine consecutive days. After being treated for nine consecutive days (days 1–9), all rats except group I received scopolamine hydrochloride (1.5 mg/kg body weight, i.p.) 30 min prior to the Morris water maze test.

The chosen dose for LP was based on the administration dosages for human being. It has been reported that transdermally administrated LP (460 mg/day) for treatment of cardiovascular diseases showed higher bioavailability in comparison with oral administration in human (25), however, there is few literature referred to the transdermal dose of LP in the treatment of AD. Based on the information above, according to the dose conversion among rats and healthy volunteers, the LP ethosomal system designed for every 3 day's clinical application was adopted in the pharmacodynamic study, for long-term AD prevention.

Morris Water Maze Test

The behavioral performance of the rats was evaluated in the Morris water maze (26), which consisted of a black circular water pool (120 cm diameter×45 cm height) containing water (20±1°C) to a depth of 30 cm. The pool was divided into four equal quadrants and an escape platform was hidden 1 cm below the water surface in a fixed location.

After 1-day's training (day 4) for the rats to get used to the pool, the rats were given four training trials per day for four consecutive days (days 5, 6, 7, and 8) with the escape platform hidden in the middle of the southwest quadrant. The starting position was changed randomly for each trial and each rat was allowed to swim freely until it found the submerged platform or until 120 s elapsed. If the rat found the platform, it was allowed to remain there for 15 s and then returned to its home cage. If it was unable to find the platform within 120 s, it was then placed

on the platform for 15 s and a maximum score of 120 s was assigned. In each training trial, the time to reach the platform (escape latency) was measured. On day 9, each rat was allowed to swim inside the pool 30 min after injection of scopolamine hydrochloride, and the escape latency was recorded.

Measurements of SOD, GSH-Px Activities, and MDA Levels in the Brain of Rats

After the Morris water maze test, all rats were sacrificed by cervical dislocation, and the brain was immediately removed and weighed. Before detection, the brain was rapidly homogenized in ice-cold saline at 13,000 rpm in a Potter homogenizer. The homogenate was centrifuged at 3,500 rpm at 4°C for 15 min, and the supernatant was collected for assay. SOD, GSH-Px activities, and MDA levels in the brain were determined using the respective kits (Nanjing Jiancheng Bioengineering Institute, Nanjing, People's Republic of China). Protein concentrations were assessed by the BCA assay (Cowin Biotech, Beijing, China).

Statistical Analysis

The statistical analysis was performed using OriginPro 7.5 software. Each data value is presented as the mean±standard deviation (S.D.). The data was analyzed by one-way ANOVA followed by a post hoc Bonferroni's multiple comparison test. The data were considered to be statistically significant if $P<0.05$ or less.

RESULTS

Characterization of LP Ethosomal System

LP ethosomal system was characterized for vesicle size, size distribution, entrapment efficiency, stability, and pH value. The mean size of LP ethosomes was 146.3±24.6 nm with the polydispersity index of 0.034±0.009. The drug entrapment efficiency of LP ethosomal system was found to be 70.23±1.20%. Vesicular size measurement of ethosomes stored at 4°C showed only 2.2±0.4% size increase in 4 weeks suggesting good stability of the LP ethosomal systems. The pH value of the LP ethosomal system was 5.9, being in the range of pH value for human skin, from 4.5 to 6.6 (27), indicating that the LP ethosomal system was compatible to the human skin, and its irritation to the skin was low.

In Vitro Skin Permeation Study

Depth of Skin Penetration

The cationic hydrophilic fluorescent probe R6G was used to study skin penetration from the ethosomal systems into nude mouse skin after nonocclusive application. Confocal laser scanning micrographs of the skin after 12-h application of R6G from LP ethosomal systems or aqueous systems are shown in Fig. 2.

The delivery from ethosomal systems resulted in a significant increase in both the depth of penetration (up to 200 μm) and the maximum fluorescence intensity (255 AU) as compared with the aqueous systems that were confined to low maximum fluorescence intensity (130 AU) with the depth of penetration up to 125 μm.

LP Permeation Across the Skin

The permeation profiles of LP through rat abdominal skins from the ethosomal systems and the aqueous systems followed zero-order release kinetics, respectively (Fig. 3). A steady increase of LP in the receptor chamber with time was observed. Statistical comparison of the permeation parameters throughout 24 h shown that the LP ethosomal system provided a J_s of 113.50±12.6 μg cm^{-2} h^{-1} significantly higher than the aqueous system (J_s=21.45±4.1 μg cm^{-2} h^{-1}), and T_{lag} of the LP ethosomal system (2.0 h) was shorter than that of the aqueous one (2.3 h) although there is no statistical significance between them.

The extraction of LP from the skin resulted specific and efficient, because no interference from skin components was present and the recovery rate was 92.6±13.0%. The drug deposition in skin of the LP ethosomal system (0.88±0.12 μg/g) was significantly higher than that of the LP aqueous one (0.51±0.06 μg/g).

Effect of LP Ethosomal System on Scopolamine-Induced Amnesia Rats

Morris Water Maze Test

The Morris water maze test is a sensitive method for revealing the impairment of spatial learning and memory. As shown in Fig. 4, the escape latencies of all the rats were significantly shortened during the acquisition training. Moreover, there was no significant difference in the escape latencies among the groups on the same day, indicating that LP had no effect on the normal rats.

On day 9, the rats received a scopolamine injection in order to induce memory deficits (Fig. 4). Significant differences among the groups were obtained [F (2, 12)=134.94, $P<0.001$]. The escape latency of the amnesic rats in group II was significant higher than that of the normal rats in group I [F (1, 8)=155.40, $P<0.001$]. Transdermal treatment with LP ethosomal systems totally reversed the memory deficits induced by scopolamine, with the escape latency decreasing from 104.76±11.48 s on the fifth day to 30.48±2.75 s on the ninth day, to the similar level of the normal rats (group I), with the escape latency decreasing from 103.10±11.36 s on the fifth day to 29.52±3.11 s on the ninth day.

Effects of LP Ethosomal System on SOD, GSH-Px Activities, and MDA Levels in the Brain of Rats

To elucidate the biochemical mechanism of the anti-amnesic activity for LP ethosomal system, the effects on the activities of antioxidant enzymes and the levels of MDA were determined, and the results are shown in Table I. Compared with group I, the administration of scopolamine (group II) resulted in significant reductions of SOD activities [F (1, 10)=435.44, $P<0.001$] and GSH-Px activities [F (1, 10)=152.10, $P<0.001$] in the brain, and the MDA levels were significantly increased [F (1, 10)=207.64, $P<0.001$]. Transdermal administration of LP ethosomal system (group III) totally recovered the activities of SOD and GSH-Px in the brain of the scopolamine-induced amnesia rats to the similar levels of the normal rats, and the increase in

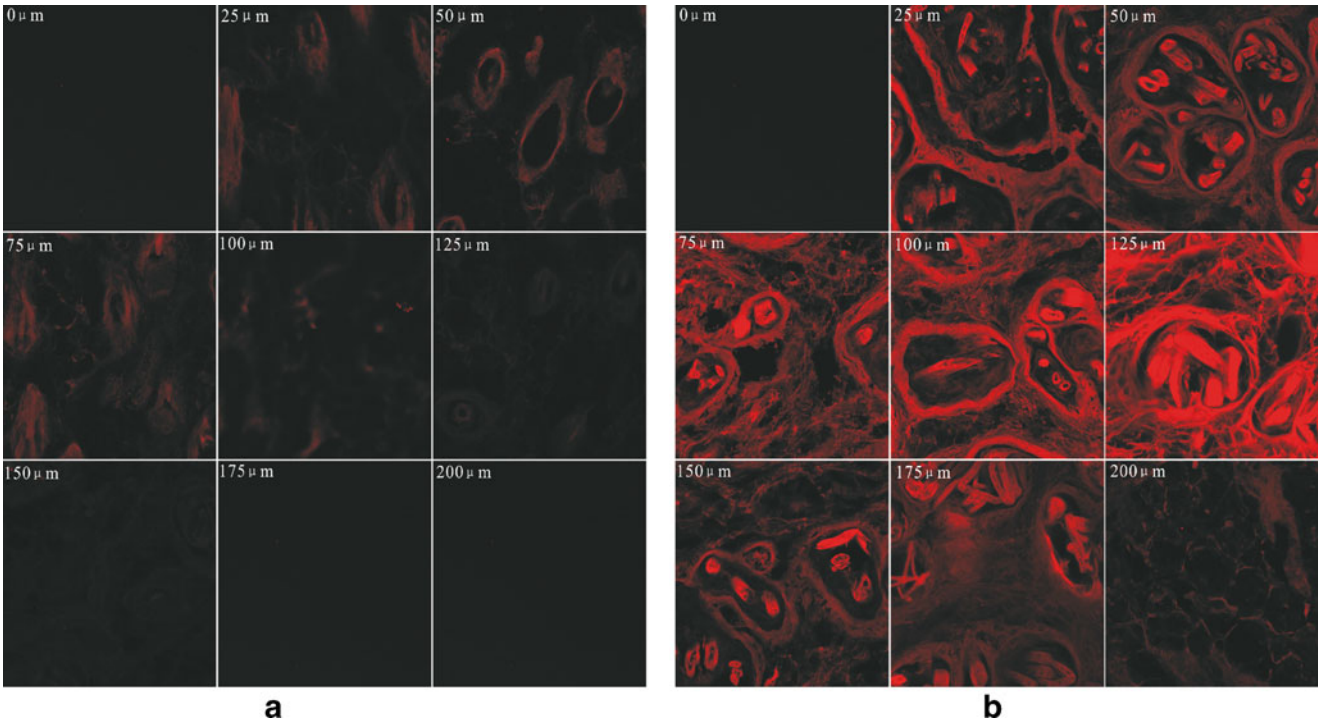

Fig. 2. CLSM micrographs of nude mouse skin after *in vitro* application of **a** LP ethosomal system and **b** LP aqueous system for 12 h. The skin was visualized by CLSM at 25-μm increments through the *Z*-axis. The full-thickness skin was divided to nine fragments from the surface of the skin (*top* to *bottom*)

MDA levels induced by scopolamine was also recovered to the similar levels of the normal rats.

DISCUSSION

To search for alternative treatments of AD is the forefront today since the current therapeutic strategies are limited to those that attenuate AD symptoms without deterring the progress of the disease itself (28).There is accumulating evidence that suggests a key role of oxidative stress in the pathophysiology of AD (29), and the successful neuronal protection from oxidative stress will therefore potentially prevent the disease altogether, if appropriately administered (28). As stated above, an effective antioxidant treatment regimen can potently buffer the impacts of oxidative stress to ultimately slow down the progression of AD.

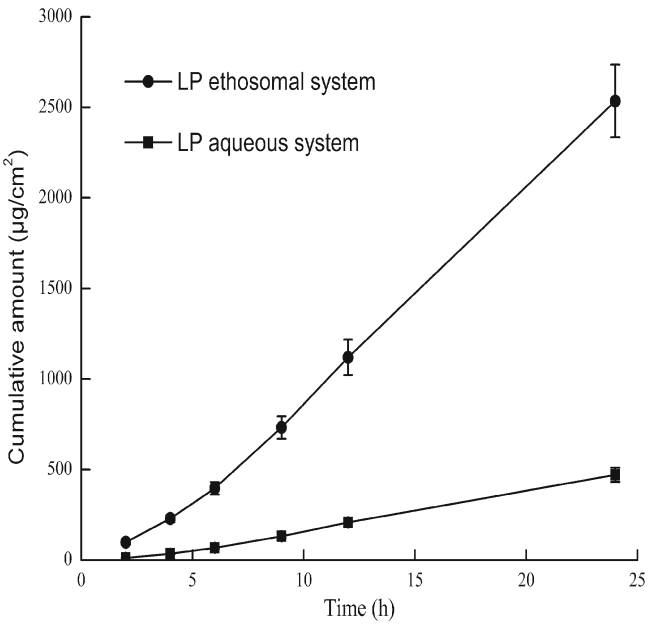

Fig. 3. The *in vitro* permeation profiles of LP through rat abdominal skins from ethosomal system and aqueous system (mean±S.D., $n=3$)

Ligustrazine is widely used in clinic for treatment of cerebrovascular and cardiovascular diseases. Improvements of learning and cognitive function by ligustrazine have been reported in rodents following D-galactose (16), nevertheless, there are few literatures referring to the pharmacological mechanisms of ligustrazine for the anti-amnesic efficiency. Keeping these processes in mind, we have hypothesized here that ligustrazine may be effective in the treatment of AD through exerting effects on the oxidative system in the brain.

Based on these findings and aiming to overcome the extensive hepatic first-pass metabolism, the variable plasma drug concentration, the multiple daily dose regimens, and the poor patient compliance associated with the LP oral or injection administration, we have constructed a LP transdermal ethosomal system, in which carbomer has been adopted to increase the viscosity of LP ethosomes, allowing for convenient administration. Ethosome, as a novel liposome, the main characteristics of which are the bilayers fluidity of the soft phospholipid vesicle in conjunction with the presence of high concentration of ethanol in the system, has a high deformability and entrapment efficiency (30), making it easy to completely penetrate through the skin and improve drug delivery. These properties are very important for ethosome as a drug carrier in the transdermal

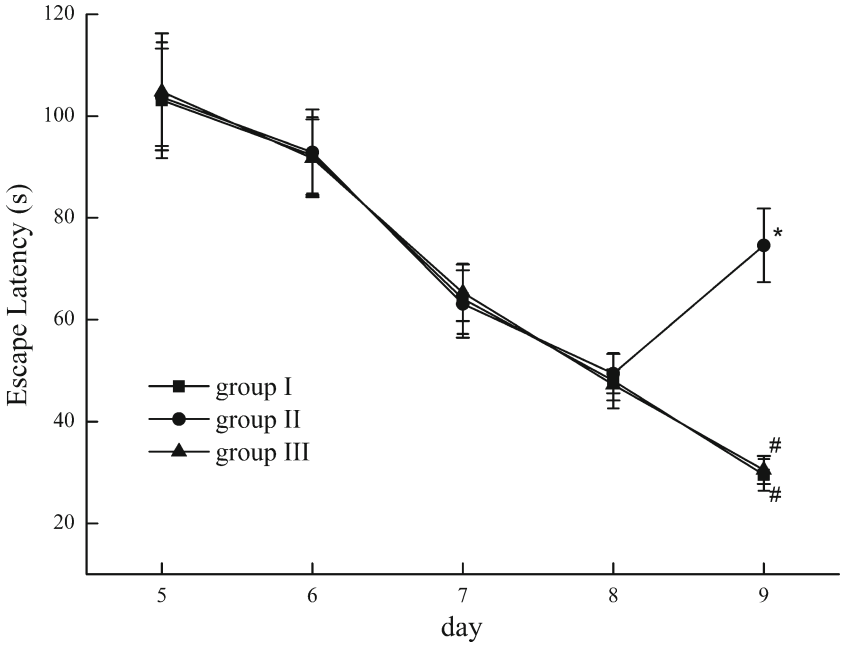

Fig. 4. The escape latency of rats in group I (*black square*), group II (*black circle*), and group III (*black triangle*), in the Morris water maze test. Each data point represents the mean (±S.D.) escape latency of four trails for six rats performed each day. $^{*}P<0.001$, results significantly differ from the values of group I; $^{\#}P<0.001$, results significantly differ from the values of group II

delivery system, which can provide an efficient intracellular delivery for hydrophilic drugs (31).

In terms of vesicular characterization, the vesicular size of 146.3±24.6 nm provides a sufficient opportunity for the LP ethosomal system to obtain a fine skin permeation absorption, as the penetration abilities of permeates are inversely related to the size of the ethosomes (22) and the vesicles smaller than 300 nm are able to deliver the permeates into deeper skin layers efficiently (32). Therefore, there is the potential for the ethosomal system to delivery LP through the skin. Furthermore, the designed LP ethosome has high entrapment efficiency with satisfactory stability.

When investigating the enhanced effect of LP ethosomal system on the skin delivery of R6G by CLSM, it has been found that the probe from the ethosomal system penetrates the nude mouse skin to a much greater depth than from the aqueous one. Additionally, compared with the LP aqueous system, the superior ability of the ethosomal system to transdermally deliver LP has been validated by determining the penetration parameters of LP across the rat skin as well as the skin deposition of the drug in the permeation studies. The target permeation rate of LP is tailored according to the rationale (33), a zero-order release kinetic equation as follows: $AK_0 = C_p Cl$, where A represents the area of the transdermal deliver system, K_0 represents the target permeation rate, C_p represents the effective therapeutic plasma concentration, and Cl represents the total body clearance rate. According to the published data, the C_p and Cl values for LP were 200 ng/ml and 15.7 l/h, respectively (34). Based on the permeation rate of LP in the ethosomal system, 113.50± 12.6 μg cm^{-2} h^{-1} through the rat abdominal skin, the application area would be around 28 cm^2.

Furthermore, the pharmacodynamic responses due to the transdermal administration of LP from the ethosomal system have been investigated. The scopolamine-induced amnesia rat as an animal model has been adopted in the study to evaluate the anti-amnesic efficiency. As is well known, scopolamine has been widely adopted to study cognitive deficits in experimental animals (35). In addition, the effects of the LP ethosomal system on SOD activities,

Table I. The SOD, GSH-Px Activities, and MDA Levels in the Brain of Rats in Groups I–III

Groups	SOD (U/mg protein)	GSH-Px (U/mg protein)	MDA (nmol/mg protein)
Group I	84.20±3.16[a]	108.00±7.15[a]	4.20±0.31[a]
Group II	50.52±2.38	75.39±4.33	6.90±0.34
Group III	83.00±4.14[a]	105.44±4.42[a]	4.43±0.19[a]

The values are expressed as mean±S.D. ($n=6$)
[a] Results significantly differ from the values of group II: $P<0.001$

GSH-Px activities, and MDA levels in the brain of rats have been evaluated to elucidate the biochemical mechanism of the anti-amnesic efficiency, since oxidative stress is one of the pathogeneses of AD, and these activities/levels are main biomarkers of the oxidative status.

In the Morris water maze test, performance on reference memory tasks was disrupted after the rats were treated with scopolamine. Moreover, the activities of SOD and GSH-Px decreased, and the levels of MDA increased significantly in the brain, indicating that scopolamine could trigger the oxidative stress in the brain of rats, which was in line with the previous literatures (35,36). The transdermal treatment with LP ethosomal system could significantly increase SOD and GSH-Px activities, reduce MDA levels in the brain of the scopolamine-induced amnesia rats, and most importantly, reverse these activities/levels to the similar status of the normal rats, which was also indirectly reflected by the improvement in the behavioral performance.

CONCLUSIONS

The findings of the present work suggest that LP as an antioxidant is efficient in AD treatment and is therefore worth being further investigated. The LP ethosomal system we have constructed in the work exhibits enhanced skin permeation *in vitro* and efficient pharmacodynamic responses in amnesic animal model. The anti-amnesic efficiency of this ethosomal system may not only contribute to behavioral improvement, but also slow down the progression of AD by mitigating the oxidative stress. In summary, LP might offer a potential alternative therapeutic drug for the treatment of AD, and ethosomes could be vesicles of choice for transdermal delivery of LP.

ACKNOWLEDGMENTS

This work was supported by the National Science Fund of China (no. 30500666) and the Tsinghua—Yuyuan Medical Funds (no. 20240000529, no. 20240000548). The authors would like to thank Prof. Lei Huang (Department of Medicine, Tsinghua University, China) for providing the CLSM platform and the technical assistance.

REFERENCES

1. Brookmeyer R, Johnson E, Ziegler-Graham K, Arrighi HM. Forecasting the global burden of Alzheimer's disease. Alzheimer's Dementia. 2007;3:186–91.
2. Armstrong RA. Plaques and tangles and the pathogenesis of Alzheimer's disease. Folia Neuropathol. 2006;44:1–11.
3. Portelius E, Zetterberg H, Andreasson U, Brinkmalm G, Andreasen N, Wallin A, *et al.* An Alzheimer's disease-specific β-amyloid fragment signature in cerebrospinal fluid. Neurosci Lett. 2006;409:215–9.
4. Cummings JL. Alzheimer's disease. N Engl J Med. 2004;351:56–7.
5. Cai Z, Yan Y, Sun S, Zhang J, Huang L, Yan L, *et al.* Upregulation of BACE1 and β-Amyloid protein mediated by chronic cerebral hypoperfusion contributes to cognitive impairment and pathogenesis of Alzheimer's disease. Neurochem Res. 2009; 34:1226–35.
6. Zhu X, Raina AK, Perry G, Smith MA. Alzheimer's disease: the two-hit hypothesis. Lancet Neurol. 2004;3:219–26.
7. Valko M, Leibfritz D, Moncol J, Cronin MTD, Mazur M, Telser J. Free radicals and antioxidants in normal physiological functions and human disease. Int J Biochem Cell Biol. 2007;39:44–84.
8. Gu F, Zhu M, Shi J, Hu Y, Zhao Z. Enhanced oxidative stress is an early event during development of Alzheimer-like pathologies in presenilin conditional knock-out mice. Neurosci Lett. 2008; 440:44–8.
9. Zhang XL, Jiang B, Li ZB, Hao S, An LJ. Catalpol ameliorates cognition deficits and attenuates oxidative damage in the brain of senescent mice induced by D-galactose. Pharmacol Biochem Behav. 2007;8:64–72.
10. Jeong EJ, Ma CJ, Lee KY, Kim SH, Sung SH, Kim YC. KD-501, a standardized extract of *Scrophularia buergeriana* has both cognitive-enhancing and antioxidant activities in mice given scopolamine. J Ethnopharmacol. 2009;121:98–105.
11. Xu H, Shi DZ. The clinical applications and pharmacologic effects of Ligustrazine. Chin J Integr Tradit West Med. 2003;23:376–7.
12. Zhang SJ, Wang ZT, Han LH, Chai SB. Effects of tetramethylpyrazine injection on angiogenesis and expression of VEGF mRNA in ischemic myocardium of rats with myocardial infarction. Chin J Exp Tradit Med Formulae. 2011; 17:170–3.
13. Zhu XL, Xiong LZ, Wang Q, Liu ZG, Ma X, Zhu ZH, *et al.* Therapeutic time window and mechanism of tetramethylpyrazine on transient focal cerebral ischemia/reperfusion injury in rats. Neurosci Lett. 2009;449:24–7.
14. Fan LH, Wang KZ, Cheng B, Wang CS, Dang XQ. Anti-apoptotic and neuroprotective effects of tetramethylpyrazine following spinal cord ischemia in rabbits. BMC Neurosci. 2006;7:48–52.
15. Cheng XR, Zhang L, Hu JJ, Sun L, Du GH. Neuroprotective effects of tetramethylpyrazine on hydrogen peroxide-induced apoptosis in PC12 cells. Cell Biol Int. 2007;31:438–43.
16. Zhao L, Wei MJ, He M, Jin WB, Zhao HS, Yao WF. The effects of tetramethylpyrazine on learning and memory abilities of mice with Alzheimer disease and its possible mechanism. Chin Pharmacol Bull. 2008;24:1088–92.
17. Wang L, Guo Q, Han J, Zhang Y, Chen X. Pharmacokinetics of ligustrazine in blood, brain, and liver of mice. Chin Tradit Herb Drugs. 2009;40:935–8.
18. Cai W, Dong SN, Lou YQ. HPLC determination of tetramethylpyrazine in human serum and its pharmacokinetic parameters. Acta Pharmaceut Sin. 1989;24:881–6.
19. Zeng CY, Mei QX. ADRs induced by tetramethylpyrazine: literature analysis of 30 cases. China Pharm. 2008;19:1908–10.
20. Prausnitz MR, Mitragotri S, Langer R. Current status and future potential of transdermal drug delivery. Nat Rev Drug Discov. 2004;3:115–24.
21. Shakeel F, Baboota S, Ahuja A, Ali J, Aqil M, Shafiq S. Nanoemulsions as vehicles for transdermal delivery of aceclofenac. AAPS PharmSciTech. 2007;8:191–9.
22. Fang YP, Tsai YH, Wu PC, Huang YB. Comparison of 5-aminolevulinic acid-encapsulated liposome *versus* ethosome for skin delivery for photodynamic therapy. Int J Pharm. 2008;356:144–52.
23. Mishra D, Mishra PK, Dabadghao S, Dubey V, Nahar M, Jain NK. Comparative evaluation of hepatitis B surface antigen-loaded elastic liposomes and ethosomes for human dendritic cell uptake and immune response. Nanomedicine. 2010;6:110–8.
24. Lopez-Pinto JM, Gonzalez-Rodriguez ML, Rabasco AM. Effect of cholesterol and ethanol on dermal delivery from DPPC liposomes. Int J Pharm. 2005;298:1–12.
25. Shen T, Xu H, Weng W, Zhang J. Study on the human pharmacokinetics and relative bioavailability of tetramethylpyrazine

phosphate patch. Proceedings of the sixth Chinese pharmaceutical association annual meeting. 2006, Nov 9, Guangzhou, China.
26. Sethi P, Jyoti A, Hussain E, Sharma D. Curcumin attenuates aluminium-induced functional neurotoxicity in rats. Pharmacol Biochem Behav. 2009;93:31–9.
27. Zhang LW, Al-Suwayeh SA, Hsieh PW, Fang JY. A comparison of skin delivery of ferulic acid and its derivatives: evaluation of their efficacy and safety. Int J Pharm. 2010;399:44–51.
28. Schenk D. Current challenges for the successful treatment and prevention of Alzheimer's disease: treating the pathologies of the disease to change its clinical course. Alzheimer's Dementia. 2008;4:S119–21.
29. Butterfield DA, Perluigi M, Sultana R. Oxidative stress in Alzheimer's disease brain: new insights from redox proteomics. Eur J Pharmacol. 2006;545:39–50.
30. Dubey V, Mishra D, Jain NK. Melatonin loaded ethanolic liposomes: physicochemical characterization and enhanced transdermal delivery. Eur J Pharm Biopharm. 2007;67:398–405.
31. Elsayed MMA, Abdallah OY, Naggar VF, Khalafallah NM. Deformable liposomes and ethosomes: mechanism of enhanced skin delivery. Int J Pharm. 2006;332:60–6.
32. Verma DD, Verma S, Blume G, Fahr A. Particle size of liposomes influences dermal delivery of substances into skin. Int J Pharm. 2003;258:141–51.
33. Zhao JH, Fu JH, Wang SM, Su CH, Shan Y, Kong SJ, *et al*. A novel transdermal patch incorporating isosorbide dinitrate with bisoprolol: *in vitro* and *in vivo* characterization. Int J Pharm. 2007;337:88–101.
34. Qi X, Ackermann C, Sun D, Sheng M, Hou H. Physicochemical characterization and percutaneous delivery of 2,3,5,6-tetramethylpyrazine. Int J Pharm. 2003;253:177–83.
35. Chen J, Long Y, Han M, Wang T, Chen Q, Wang R. Water-soluble derivative of propolis mitigates scopolamine-induced learning and memory impairment in mice. Pharmacol Biochem Behav. 2008; 90:441–6.
36. Fan Y, Hu J, Li J, Yang Z, Xin X, Wang J, *et al*. Effect of acidic oligosaccharide sugar chain on scopolamine-induced memory impairment in rats and its related mechanisms. Neurosci Lett. 2005;374:222–6.